processes

MDPI

Article

Study on Water Intake Characteristics and Influencing Parameters of Drinking Water Emergency Extraction Vehicle

Yaoqing Hou, Gangyan Li *, Hanwei Bao, Ran Zhao and Wen Zhang

School of Mechanical and Electrical Engineering, Wuhan University of Technology, Wuhan 430070, China
* Correspondence: gangyanli@whut.edu.cn; Tel.: +86-138-0716-6765

Abstract: In this paper, by analyzing the heat and mass transfer characteristics of the dehumidification runner microelement channel of a drinking water emergency extraction vehicle, a mathematical model of heat and mass transfer in the water intake process is established, and the influence of the runner parameters (adsorbent thickness, regeneration angle, rotation speed) and air parameters (treatment air temperature/humidity, regenerated air temperature/humidity) on the water intake characteristics is mainly studied. Water extraction experiments are carried out in arid desert areas and humid island environments. The test results showed that compared with the calculated data, the deviations in the temperature and humidity of the treated air outlet were 3.03% and 4.14%, respectively, and the deviation value of the water intake was 8.23% when the moisture content of the inlet air was 2 g/kg.

Keywords: drinking water emergency extraction vehicle; water intake characteristics; mathematical model; verification test

check for updates

Citation: Hou, Y.; Li, G.; Bao, H.; Zhao, R.; Zhang, W. Study on Water Intake Characteristics and Influencing Parameters of Drinking Water Emergency Extraction Vehicle. *Processes* **2023**, *11*, 555. https://doi.org/10.3390/pr11020555

Academic Editor: Anna Trubetskaya

Received: 7 December 2022
Revised: 3 February 2023
Accepted: 8 February 2023
Published: 10 February 2023

Copyright: © 2023 by the authors. Licensee MDPI, Basel, Switzerland. This article is an open access article distributed under the terms and conditions of the Creative Commons Attribution (CC BY) license (https://creativecommons.org/licenses/by/4.0/).

1. Introduction

Water is one of the most precious resources in the world, and the shortage of fresh water is a problem worldwide. However, air water intake, which is not restricted by region, has the advantages of strong adaptability and less restrictions with regard to the environment, and it is one of the most effective means to solve the issue of the shortage of fresh water. Biswas et al., analyzed the worldwide water crisis [1], and Salehi et al., have suggested that there is a maximum water reserve in the air [2]. Tu et al., summarized the working principles, performance and test setup or simulation methods of various air extraction technologies, comparing and evaluating these [3]. The most commonly used methods for extracting water from air include cooling and condensation extraction, mist extraction and adsorption extraction. Patel et al., developed a condensing water extraction device and conducted experimental studies under seven different climatic conditions [4]. Kandeal et al., conducted a comparative analysis of the factors affecting air water extraction for cooling condensation and adsorption methods [5]. Shafeian et al., summarized and discussed different water extraction technologies and looked forward to the development of air water extraction technologies [6]. Raveesh summarized and compared the performances of various water extraction technologies in terms of important performance parameters, constraints, etc. [7]. In recent years, there has been much research on the adsorption mechanism, the improvement of adsorption performance, the relationship between adsorption capacity and the air state, and developing a matching adsorbent and condensation system. Toribio et al., elucidated the adsorption mechanism of hydrophilic polymer and its adsorption performance [8]. Seo et al., developed a layered porous metal adsorption material with a good dehumidification performance [9]. Tao et al., analyzed the adsorption/desorption performance of a molecular sieve desiccant using a comparative method [10]. Hao et al., conducted a study on the matching of a dehumidification rotor and a condensing system [11]. At the same time, Zhang et al., focused on the matching

characteristics of heat transfer processes and coupled heat and mass transfer processes to optimize system performance [12]. Ge et al., studied the heat and mass transfer mechanism and a modeling method [13]. Zhang et al., analyzed temperature and humidity distribution inside a dehumidification runner and the heat and mass transfer coupling relationship [14]. Hao and Eslami analyzed the relationship between dehumidification capacity and energy consumption under different influencing factors [15,16]. In order to improve the efficiency of water intake, research has recently been carried out in the areas of solar air intake and semiconductor refrigeration water intake. Chen et al., conducted an analytical summary of solar-powered adsorption/desorption atmospheric water collection technologies [17]. Kim et al., developed a device to implement air extraction using low-grade heat from natural sunlight [18]. Abdelgaied et al., conducted an experimental study to improve the performance of adsorption air-conditioning systems using solar reheating technology [19]. Ge et al., conducted a comparative analysis of energy consumption in dehumidification systems with solar energy alone and with a mixture of conventional and solar energy sources [20]. Pang et al., conducted a theoretical analysis of the optimum state for obtaining high cooling capacity with low power from semiconductors and deduced a theoretical formula for the optimum current [21]. Wei et al., conducted a comprehensive analysis of energy savings in solar semiconductor condensing wall water extraction systems [22].

A drinking water emergency intake water-making vehicle can obtain drinking water in various complicated situations with air water and surface water purification. Possible circumstances include: (1) in a desert or other area in which there is no surface water area, runner water can be used; (2) air condensation can be used for water intake in islands and coastal areas with high moisture content; (3) reverse osmosis can be used for water purification in areas with surface water.

The existing research focuses on adsorption materials, channel shapes, hygroscopic properties and other aspects of laboratory simulation, but the various parameters of systematic study and physical verification are relatively small. In this paper, a theoretical analysis of the changes in the state of the adsorbent temperature, adsorption rate, air temperature and humidity within the micro-element channel of a dehumidification runner is carried out. On this basis, the influence of the runner's parameters and the air parameters with regard to the water intake characteristics of the equipment is addressed, the processes of heat and mass transfer are analyzed, and a mathematical model is constructed. The parameters are simulated and optimized, and their accuracy is verified by experiments. In contrast to other existing studies, this paper presents a systematic analysis of the key parameters affecting the water extraction characteristics of the rotor and the constraints between such parameters, providing theoretical support for the study of the runner water intake device to implement accurate control of the various parameters, in order to improve the water intake rate and to reduce energy consumption.

2. Materials and Methods

The emergency drinking water production vehicle adopts a rotary wheel system of air water intake, which is composed of a runner, a fan, an evaporator, a regeneration heater, etc. The system includes two parts, the first of which is the treatment process. When natural air enters the treatment area, the air water molecules are adsorbed by the hygroscopic agent inside the runner, and after the runner has adsorbed the water molecules and become saturated, it turns to the regeneration area with the runner and enters the regeneration process. In the regeneration process, regeneration air is heated by the heater to a predetermined temperature and reversed through the regeneration area of the runner. In the high-temperature state of the water molecules being adsorbed by the runner, they are desorbed and distributed to regeneration air, and the regeneration air creates a larger moisture content in saturated wet air. The saturated wet air enters the condensing air duct of the water extraction system through the regeneration fan. As the water in the adsorbent is desorbed and taken away, the moisture absorption capacity of the adsorbent is restored. At the same time, the runner rotates slowly at a low speed of 8~15 r/h (which can be regarded

as an inertial system), thus ensuring the continuity of moisture absorption/desorption. The desorbed saturated moist air enters the condensation channel to cool and completes the air intake process, as shown in Figure 1.

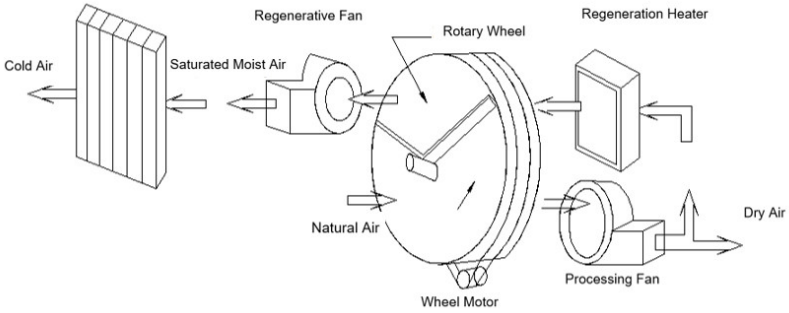

Figure 1. Schematic diagram of rotary air intake system.

For the adsorption characteristics of the quantitative analysis runner, a Lagrange cylindrical coordinate system is established for an air microchannel in the runner, as shown in Figure 2. In a cycle of the runner's rotation, through the analysis of a micro-channel, the process of change is described for the entire water intake runner's working state.

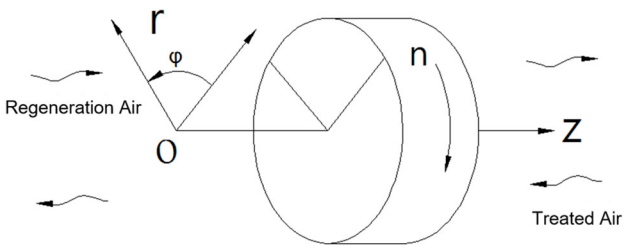

Figure 2. Schematic diagram of the mathematical model of the rotor.

The hygroscopic/desorption performance of the runner is mainly affected by the parameters of the runner and the state of the air, and the heat and mass transfer processes of the runner are coupled with each other. According to the actual shape of the runner's air passage, a mathematical model of heat and mass transfer is established by setting reasonable boundary conditions, and the model is verified by test data. Analyzing the runner's performance through numerical calculation is an effective method to improve the hygroscopicity and desorption of the runner.

Considering the heat and mass transfer area of water molecules in the channel and the difficulty of runner processing, the cross section of the micro channel is in the shape of sine wave, as shown in Figure 3.

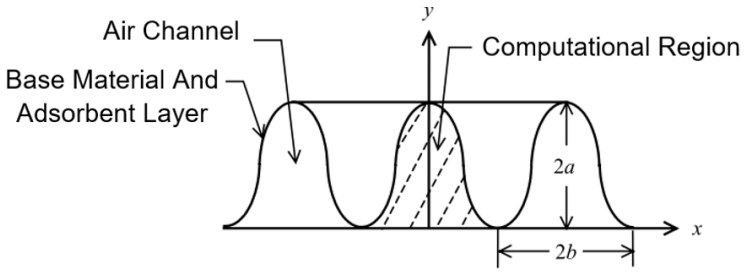

Figure 3. Corrugated air passage.

Based on the small cross-sectional size of the microelement channel and the thickness of the adsorbent coating, the structure and material are consistent and evenly distributed in the single microelement DZ, as shown in Figure 4. The lumped parameter method can be

used to analyze the heat and mass transfer process of water molecules in the microchannel, and a one-dimensional heat and mass transfer mathematical model of the microchannel can be established.

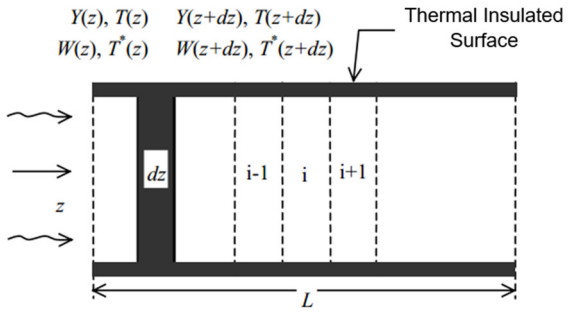

Figure 4. Computational grid.

Under actual working conditions, the adsorption capacity of the rotor substrate for water is negligible compared to that of the adsorbent, and the central wall of the rotor substrate is nearly adiabatic. For the purposes of analysis, the physical properties of dry air and water vapor are assumed to be constant, and molecular diffusion and thermal conductivity in the axial direction as well as the influence of the adsorbent moisture desorption process on the thickness of the heat and mass transfer boundary layer are ignored [13].

Based on mass and conservation of energy, the following transfer and conservation equations can be obtained.

(1) The mass conservation equation between air and adsorbent is as follows:

$$\frac{\partial Y}{\partial t} + \nu\frac{\partial Y}{\partial z} + \frac{\rho_{ld}}{2A\rho_\alpha}\frac{\partial W}{\partial t} = 0 \tag{1}$$

where Y is the moisture content of air, W is the adsorption amount of desiccant, ρ_{ld} is the desiccant mass per unit length, ρ_α is the dry air density, and W is the channel cross-sectional area.

(2) The mass transfer equation of adsorbent side is expressed as:

$$\frac{\partial W}{\partial t} + \frac{2K_y l}{\rho_{ld}}(Y_w - Y) = 0 \tag{2}$$

where K_y is the mass transfer coefficient, and l is the channel cross-sectional circumference.

(3) The energy conservation equation between the air and the adsorbent is:

$$\frac{\partial \theta}{\partial t} + \nu\frac{\partial \theta}{\partial z} + \frac{\rho_{ld}\left(c_{pd} + Wc_{pl}\right) + \rho_{lm}c_{pm}}{2A\rho_\alpha\left(c_{pa} + Yc_{pv}\right)}\frac{\partial \theta^*}{\partial t} = \frac{K_y Q l}{A\rho_\alpha\left(c_{pa} + Yc_{pv}\right)}(Y - Y_w) \tag{3}$$

where θ is the c_{pm} air temperature, θ^* denotes the desiccant temperature, c_{pd} is the constant pressure specific heat of the molecular sieve, c_{pl} is the constant pressure specific heat of saturated water, $Y^{c_{pm}}$ is the constant pressure specific heat of dry air, c_{pv} is the constant pressure specific heat of dry saturated water vapor, ρ_{lm} is the line mass of the substrate in a single channel, and W is the amount of desiccant adsorption.

(4) The heat transfer equation of adsorbent side can be expressed as:

$$\frac{\partial \theta^*}{\partial t} + w_1(\theta^* - \theta) + w_2(Y_w - Y) + w_3(Y_w - Y)(\theta - \theta^*) = 0 \tag{4}$$

where $w_1 = \frac{2\alpha l}{\rho_{ld}\left(c_{pd}+Wc_{pl}\right)+\rho_{lm}c_{pm}}$, $w_2 = \frac{2K_y Q l}{\rho_{ld}\left(c_{pd}+Wc_{pl}\right)+\rho_{lm}c_{pm}}$, $w_3 = \frac{2K_y c_{pv} l}{\rho_{ld}\left(c_{pd}+Wc_{pl}\right)+\rho_{lm}c_{pm}}$, and α is the coefficient of convective heat transfer.

Equations (1)–(4) are written as implicit upwind difference equations with backward differences for both temporal and spatial derivatives, which are then solved by MATLAB. The initial and boundary conditions are set as follows.

Initial conditions:

$$\theta(z,0) = \theta_0$$

$$Y(z,0) = Y_0$$

$$\theta^*(z,0) = \theta^*{}_0$$

$$W(z,0) = W_0$$

$$Y_w(z,0) = Y_{w0}$$

Boundary conditions:

$$\theta(0,t) = \begin{cases} \theta_{reg}, For\ the\ regeneration\ process \\ \theta_{ads}, For\ the\ dehumidification\ process \end{cases}$$

The heat of adsorption Q and the moisture content of the wet air on the desiccant surface $Y_W(\theta^*,W)$ involved in the above equation are determined by the following relationship.

The heat of adsorption Q equation is:

$$Q = L_v[1.0 + 0.2843\exp(-10.28W)]$$

where L_v is the latent heat of evaporation of saturated water ($J{\cdot}kg^{-1}$).

The saturation sorption equation is expressed as:

$$\varphi_w = 0.0078 - 0.05759W + 24.16554W^2 - 124.78W^3 + 204.226W^4$$

Anthony's saturated water vapor pressure equation is:

$$P_{ws} = \exp\left(23.196 - \frac{3816.44}{\theta^* - 46.13}\right)$$

The conversion relationship between the moisture content of wet air and the relative humidity is:

$$Y_w = \frac{0.622p_w}{p_{atm} - p_w} = \frac{0.622\varphi_w}{p_{atm}/p_{ws} - \varphi_w}$$

In addition, the heat and mass transfer coefficients for the treatment and regeneration processes are determined by the following three equations, respectively:

$$Nu_z = Sh_z$$

$$\alpha = \frac{Nu_2\lambda l}{4A}$$

$$K_y = \rho_\alpha \frac{Sh_z Dl}{4A}$$

In this study, a highly efficient composite adsorbent material with high stability and outstanding moisture absorption/desorption performance, that is, a 13X molecular sieve ($Na_2O{\cdot}Al_2O_3{\cdot}2.45SiO_2{\cdot}6.0H_2O$), was chosen as the adsorbent material. The initial parameters used for the calculation of the heat and mass transfer mathematical model of the rotor are shown in Table 1.

Table 1. Initial parameters for the calculation of the mathematical model of heat and mass transfer of the rotor.

Name	Numerical Value
Regeneration air inlet temperature θ_{reg} (°C)	130
Treated air inlet temperature θ_{ads} (°C)	25
Treated air inlet humidity $ø_{ads}$ (%)	29.14
Reclaimed air flow rate V_{reg} ($m \cdot s^{-1}$)	1.5
Treatment air flow rate V_{reg} ($m \cdot s^{-1}$)	2.0
Specific constant pressure heat capacity of molecular sieve c_{pd} ($J \cdot kg^{-1} \cdot K^{-1}$)	0.92×10^3
Specific heat at constant pressure of the base material c_{pm} ($J \cdot kg^{-1} \cdot K^{-1}$)	0.9×10^3
Line mass ρId of desiccant on in a single channel ρ_{Id} ($kg \cdot m^{-1}$)	5×10^{-3}
Line mass ρIm ($kg \cdot m^{-1}$) of the base material in a single channel ρ_{Im} ($kg \cdot m^{-1}$)	3×10^{-3}
Channel half-height h (m)	1.5×10^{-3}
Channel half-width b (m)	1.5×10^{-3}
Aspect ratio $\gamma = 2h/b$	2
Nusser number Nu_z	2.45
Sherwood number Sh_z	2.45
Runner thickness δ (m)	0.2
Rotor radius r (m)	0.6
Rotational speed n ($r \cdot min^{-1}$)	0.25
Thermal conductivity of dry air at 100 °C λ ($w \cdot m^{-1} \cdot K^{-1}$)	3.21×10^{-2}
Constant pressure specific heat of dry air at 100 °C c_{pm} ($J \cdot kg^{-1} \cdot K^{-1}$)	1.01×10^3
Constant-pressure specific heat of dry saturated water vapor at 100 °C c_{pv} ($J \cdot kg^{-1} \cdot K^{-1}$)	2.03×10^3
Constant pressure specific heat of saturated water at 60 °C c_{pl} ($J \cdot kg^{-1} \cdot K^{-1}$)	4.18×10^3
Latent heat of evaporation of saturated water at 60 °C L_v ($J \cdot kg^{-1}$)	2.36×10^6

3. Simulation Analysis of the Parameters Influencing the Water Extraction Characteristics of Emergency Drinking Water Extraction Vehicles

3.1. Analysis of Rotor Moisture Absorption/Desorption Performance Parameters

The working state of the water extraction rotor is described by analyzing the change in air temperature, humidity and sorbent temperature in one micro-element channel, and the start of the regeneration process is taken as the starting point of the model calculation. The curves for 20 s, 40 s and 60 s are within the regeneration zone; the curves for 80 s, 120 s, 180 s and 240 s are within the treatment zone.

As shown in Figure 5, at any point in the regeneration zone, the air temperature tends to decrease along the thickness of the rotor, and the air temperature increases over time at

any point in the micro-element channel; the air temperature in the treatment zone changes in the opposite direction.

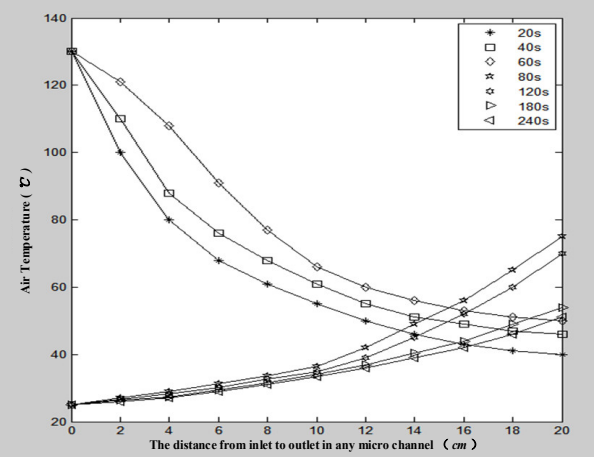

Figure 5. Variation in air temperature at various points along the channel direction.

As shown in Figure 6, the adsorbent temperature tends to increase along the thickness of the rotor in the treatment zone, and the air temperature decreases with time at any point in the micro-element channel; the opposite trend is observed in the regeneration zone.

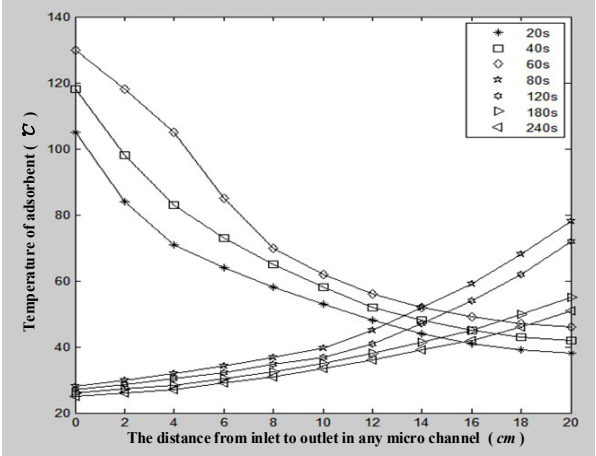

Figure 6. Change in adsorbent temperature at various points along the channel direction.

As shown in Figure 7, the humidity of the regenerated air increases at the beginning of the regeneration zone (20 s, for example), reaches a certain maximum value and then gradually decreases, and the maximum value of the regenerated air humidity gradually moves from the inlet to the outlet over time, finally reaching a maximum at the outlet, rather than reaching a maximum at the outlet at any one time.

3.2. Analysis of the Influence of Runner Structure Parameters on Water Intake Performance

3.2.1. Thickness

As shown in Figure 9, with the increase in the runner's thickness, the average value of air humidity at the regeneration side outlet increases, and the average value of air humidity at the treatment side outlet decreases. However, when the thickness increases to a certain extent, the runner's dehumidification effect is not significantly improved, but it will increase the runner's mass and energy consumption. For the convenience of calculation, the thickness of the runner is 20 cm.

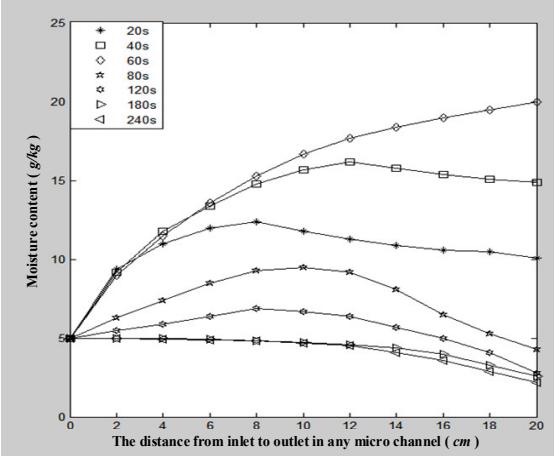

Figure 7. Change in air moisture content at various points along the passage.

As shown in Figure 8, the water adsorption rate of the adsorbent at any point in the regeneration zone gradually increases from entry to exit, and the adsorption rate of the adsorbent at any point in the micro-element channel gradually decreases with time; the rule of variation is the opposite in the treatment zone.

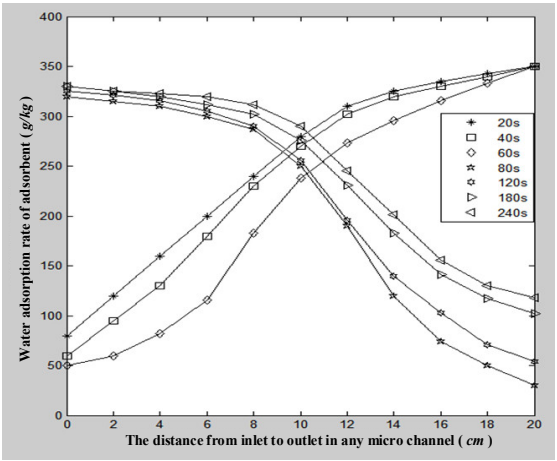

Figure 8. Variation in sorbent moisture adsorption rate at various points along the channel direction.

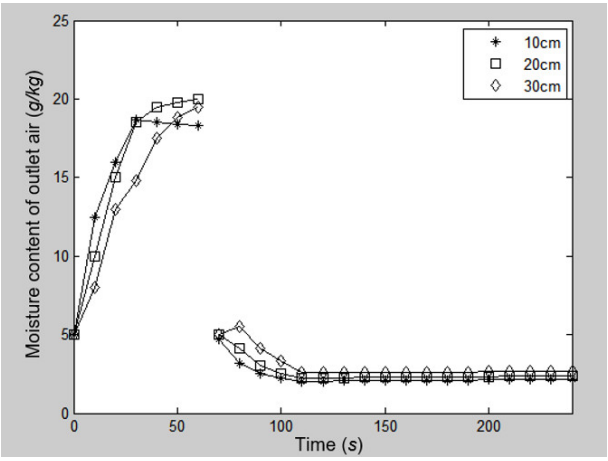

Figure 9. Change in air moisture content with time at the outlet of runner with different thicknesses.

3.2.2. Speed

The adsorption performance of the runners of different thicknesses at different speeds (regeneration angle of 90°) is reflected by the simulation solution, as shown in Figure 10. It can be seen from the graph that the runner with different thicknesses corresponds to an optimal speed. When the wheel thickness is in the range of 0.15~0.30 m, the optimal speed of 15 r/h is reached.

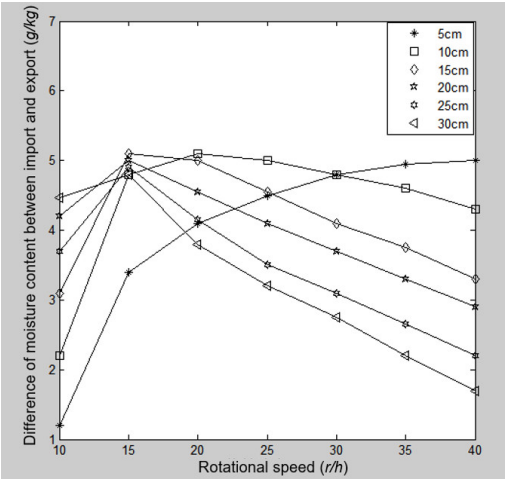

Figure 10. Effect of runner's speed on adsorption performance.

3.2.3. Regeneration Angle

The regeneration angle of the runner directly affects the hygroscopic/desorption time of the channel. As can be seen from Figure 11, for a certain thickness of the runner, there are the same optimal rotational speed values under different regenerative angles, that is, the optimal rotational speed of the runner is independent of the regenerative angle and only depends on its thickness. For a 20 cm-thick wheel, the rotating speed of 15 r/h is a cut-off point, so for the 20 cm-thick wheel, the fan angle of the regeneration zone is chosen to be 90°, leaving enough space for the treatment zone.

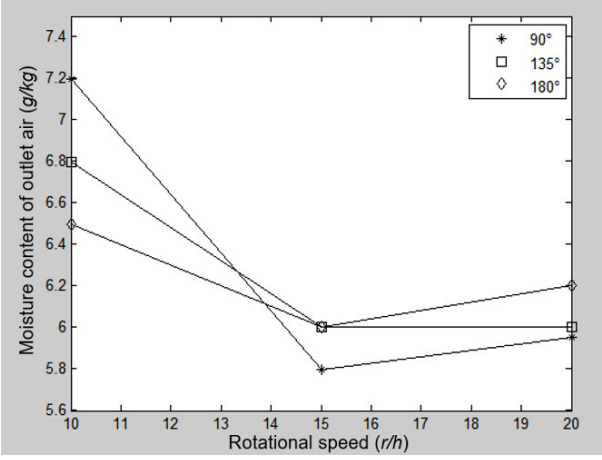

Figure 11. Effect of regeneration angle on adsorption performance (runner thickness: 20 cm).

3.3. Analysis of Influence of Air Parameters on Water Intake Characteristics

The heat and mass transfer process of a rotor is simultaneous and mutually coupled. For a given basic size and parameter of the rotor, the moisture absorption/desorption capacity is in turn related to numerous factors, such as the air temperature and moisture content at the inlet of the regeneration zone, the air temperature and moisture content

at the inlet of the treatment zone and the regeneration and treatment air velocity. An enthalpy-moisture analysis of the air inlet and outlet of the rotor therefore allows for a quantitative description of this coupled thermal mass transfer process and an analysis of the influence of the air inlet and outlet parameters on the dehumidification performance of the rotor.

The state of the air at the inlet of the rotor can be described by an enthalpy-moisture diagram (Figure 12). In the diagram, $p1$, $p2$, $r1$ and $r2$ indicate the air state points at the inlet and outlet of the treatment and regeneration zones, respectively. $p2$* is the intersection of the enthalpy line of the air inlet to the treatment zone and the line of equal relative humidity of the air inlet to the regeneration zone, and r_2* is the intersection of the enthalpy line of the air inlet to the regeneration zone and the line of equal relative humidity of the air inlet to the treatment zone. If the adsorbent in the rotor is collectively treated, and it is assumed that its moisture absorption is only related to the relative humidity of the treated air, then the iso-relative humidity line can be considered as such, and therefore, the state points $p2$ and $r2$ of the air exiting the treatment and regeneration zones should fall into the area enclosed by $p_1 \rightarrow p_2^* \rightarrow r_1 \rightarrow r_2^* \rightarrow p_1$.

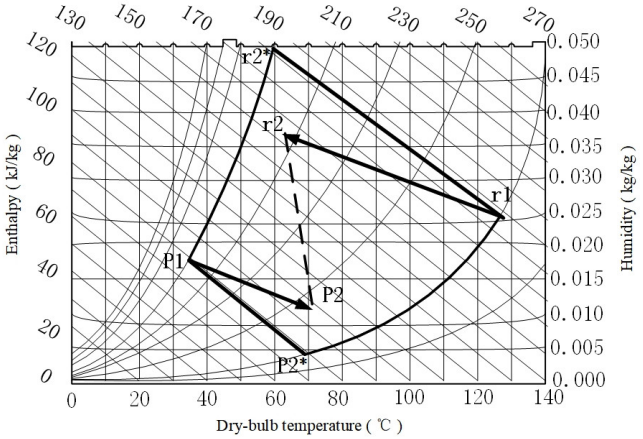

Figure 12. The state of the air in and out of the rotor on the enthalpy-moisture diagram.

The air states at the inlet and outlet should satisfy the following energy and mass conservation relationships:

$$\frac{Y_{p1} - Y_{p2}}{Y_{r2} - Y_{r1}} = \frac{\theta_r V_r}{\theta_p V_p} = \frac{h_{p2} - h_{p1}}{h_{r1} - h_{r2}}$$

where θ_p and θ_r are the angle of the treatment zone and the angle of the regeneration zone, respectively, and V_p and V_r are the head-on wind speeds in the treatment zone and the regeneration zone, respectively. From the above equation, it can be seen that $p1p2$ and r_1r_2 should be parallel, and that the line segments $\overline{p_1p_2}$ and $\overline{r_1r_2}$ simultaneously satisfy the following equation:

$$\frac{\overline{p_1p_2}}{\overline{r_1r_2}} = \frac{\theta_r V_r}{\theta_p V_p}$$

According to the above equation, as long as three of the state points are known, then the other one can be found on the enthalpy-wet diagram. For a high-performance rotor, r_1r_2 should be as close as possible to r_1r_2*, and p_1p_2 should be as close as possible to p_1p_2*, which is the overall goal and direction of the rotor's optimization. For this purpose, the dehumidification coefficient of performance, DCOP, is introduced:

$$DCOP = \frac{\dot{m}_p L(Y_{p1} - Y_{p2})}{\dot{m}_r(h_{r1} - h_{r2})}$$

where $\dot{m}_p$ and $\dot{m}_r$ are the flow rates of the air in the treatment and regeneration zones, respectively (kg/s); L is the latent heat of evaporation of water vapor (J/kg); Y_{p1} and Y_{p2} are the moisture content of the air in and out of the treatment zone, respectively (kg/kg); and h_{r1} and h_{r2} are the specific enthalpy of the air in and out of the regeneration zone, respectively (J/kg). The dehumidification coefficient of performance, DCOP, provides a comprehensive picture of the dehumidification performance and energy efficiency of the rotor by describing the variation in the air parameters at the inlet and outlet of the rotor. In fact, as shown in Figures 3–15, a higher DCOP means that r_1r_2 is closer to r_1r_2*, and p_1p_2 is also closer to p_1p_2*. For the ideal equal enthalpy dehumidification process, the DCOP tends to infinity; for the actual dehumidification process, $0 < \text{DCOP} < \infty$. Under given conditions, when the dehumidification quantity is certain, the larger the DCOP, the higher the energy utilization of the rotor and the better the dehumidification performance of the rotor. Therefore, when evaluating the dehumidification performance of a rotor, both the dehumidification capacity and the DCOP should be taken into account, and a high-performance dehumidification rotor should have both a high dehumidification capacity and a high DCOP.

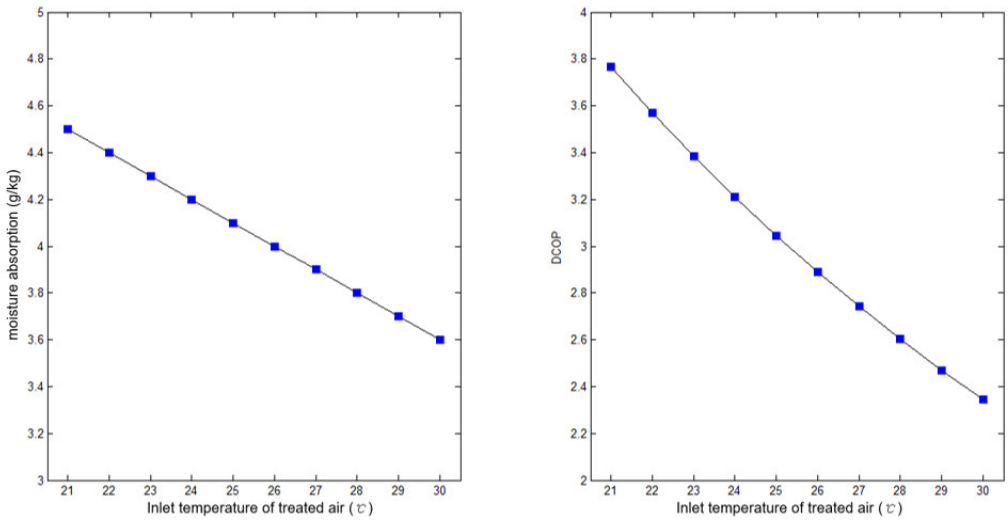

Figure 13. Effect of inlet air temperature on hygroscopicity D and DCOP.

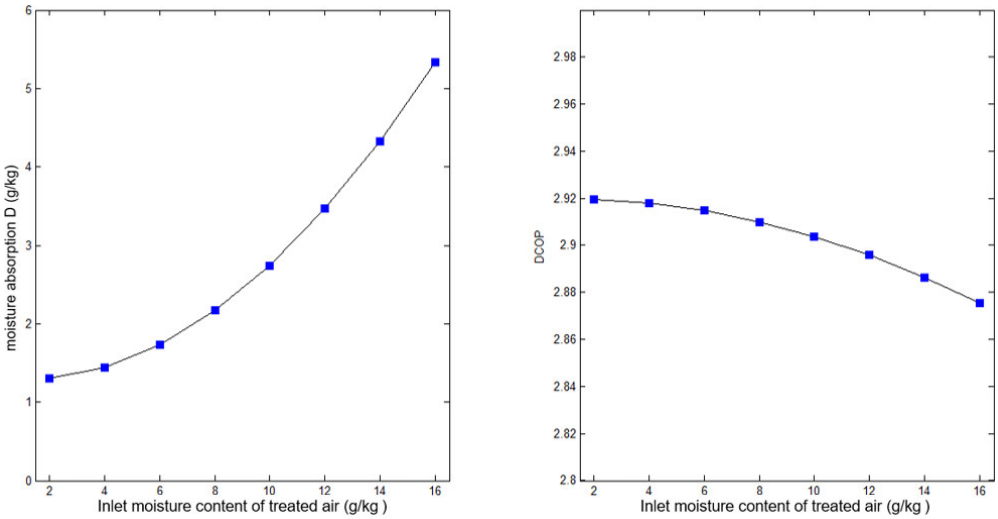

Figure 14. Effect of moisture content of air inlet on moisture absorption D and DCOP.

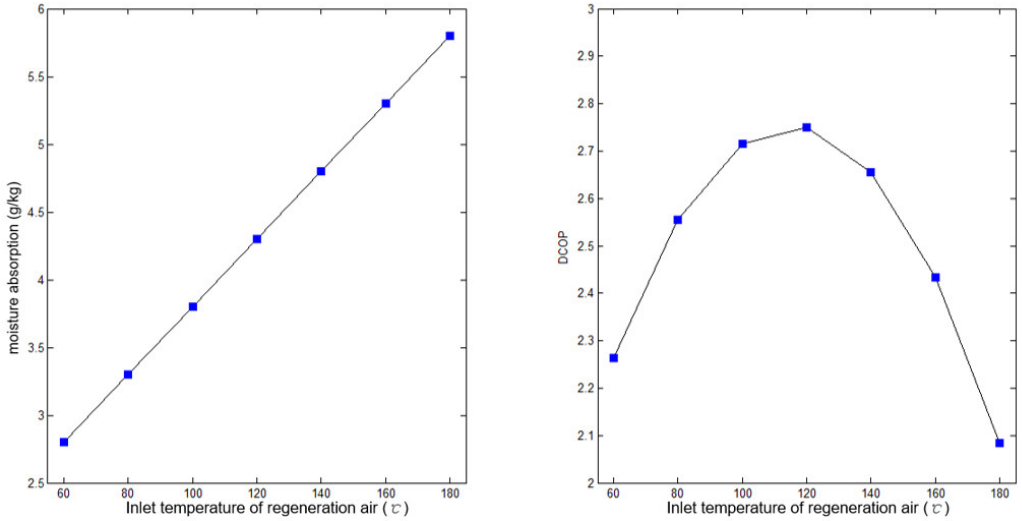

Figure 15. Effect of inlet temperature of regenerated air on hygroscopicity D and DCOP.

3.3.1. Handle Air Inlet Temperature

As shown in Figure 13, when the moisture content of the inlet air of the treatment area remains constant, with the increase in the inlet temperature of the treatment air, the moisture absorption D and DCOP of the runner decrease at the same time. The calculations show that the progressive increase in the inlet air temperature of the treatment zone reduces the adsorption capacity of the adsorbent, resulting in a reduction in the amount of moisture absorbed by the rotor; the DCOP also decreases with the increase in the inlet air temperature of the treatment zone, and the energy utilization of the rotor decreases. Under standard ambient conditions, the dehumidification performance of the rotor deteriorates when the inlet temperature of the treated air increases.

3.3.2. The Moisture Content of the Air Inlet

According to Figure 14, when other parameters are kept constant, with the increase in the moisture content of the treated air inlet, the moisture absorption capacity D of the runner increases, and the higher the moisture content of the treated air inlet, the more obvious the improvement of the moisture absorption performance of the runner. The degression value of the hygroscopicity coefficient DCOP is less than 0.06, and its influence can be neglected. Under given conditions, when the dehumidification quantity is certain, the larger the DCOP, the higher the energy utilization of the rotor and the better the dehumidification performance of the rotor. Under high humidity conditions, the runner has a higher dehumidification capacity and DCOP value, and the performance is expected to be optimal and more economical to operate.

3.3.3. Inlet Temperature of Regenerated Air

When other parameters remain unchanged, for the change in the range of the moisture absorption runner for simulation calculations, the results shown in Figure 15. It can be seen from the graph that the moisture absorption of the rotor increases with the increase in regeneration temperature when the inlet temperature of regeneration air varies from 60 °C to 180 °C, but the relationship between the DCOP and the regeneration temperature is nonlinear, i.e., there is an optimized regeneration temperature that pushes the DCOP to the maximum. In other words, a high dehumidification capacity can be achieved simply by increasing the regeneration temperature, but when it is higher than a certain optimized value, the gains will not be worth the losses in terms of energy utilization. Therefore, the regeneration temperature should not be increased blindly; otherwise, the system will consume too much energy. There is an optimal range of 110~140 °C for the regenerative air temperature of the rotor in this project. The optimum regeneration temperature range for this paper was calculated to be 130 °C.

3.3.4. Moisture Content of Regenerated Air Inlet

As can be seen from Figure 16, when the inlet moisture content of the regenerated air increases from 14 g/kg dry air to 23 g/kg dry air, the difference in the moisture absorption of the runner is only 0.27 g/kg dry air, and the desiccant performance coefficient DCOP of the runner only decreases by 0.53. It can be concluded that although the increase in the moisture content of the regenerated air inlet will reduce the wettability of the runner, the impact is small, and the inlet can be directly heated with natural air for regenerated air.

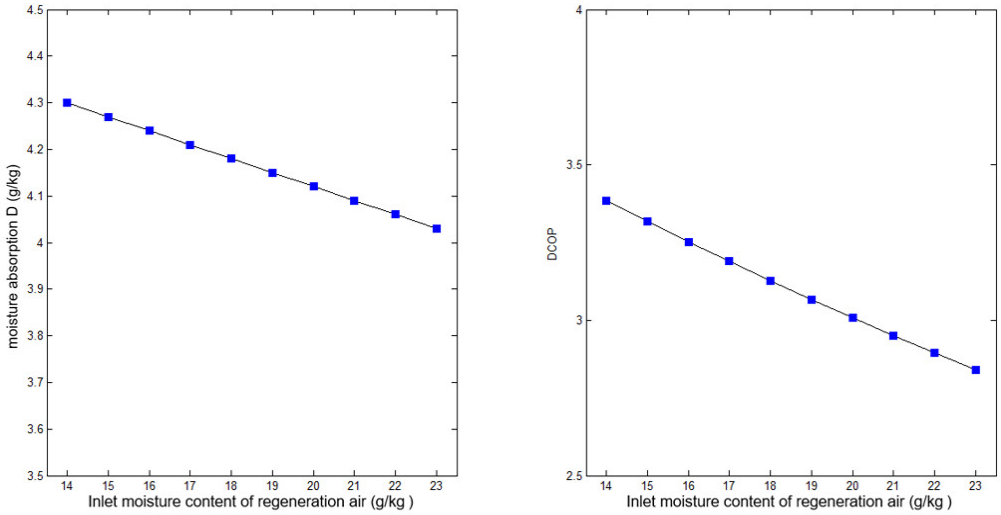

Figure 16. Effect of moisture content of regenerated air inlet on moisture absorption D and DCOP.

4. Test and Verification of Water Intake Characteristics of Emergency Drinking Water Extraction Vehicle

According to the results of the simulation analysis, the basic parameters of the emergency drinking water vehicle are determined, as shown in Table 2.

Table 2. Basic parameters of drinking water emergency extraction vehicle.

Name (Unit)	Numerical Value
Runner diameter (m)	1.2
Rotation speed (r/h)	15
Adsorbent thickness (cm)	20
Regenerative angle (°)	90
Regeneration temperature (°C)	130
Processing air volume (m^3/h)	12,000
Renewable wind volume (m^3/h)	4000

In order to verify the water intake characteristics of the wheel in different temperature and humidity environments, the emergency potable water vehicle was tested in an island environment with high air humidity and in a desert environment with very low air humidity. Experimental data at 15 °C, 11% relative humidity and 2 g/m^3 air moisture content in the desert area and 25 °C, 97% relative humidity and 18 g/m^3 air moisture content in the island environment are analyzed in comparison with data calculated based on a mathematical model.

4.1. Comparison of Moisture Content of Treated Air Outlet

As shown in Figure 17, the calculated and experimental value curves agree very well in both high and dry areas, with the two curves largely overlapping with even less deviation in the case of a high moisture content. By comparing the data, we found a maximum deviation of 4.14% between the theoretically calculated and experimentally obtained data for the moisture content of the treated air outlet.

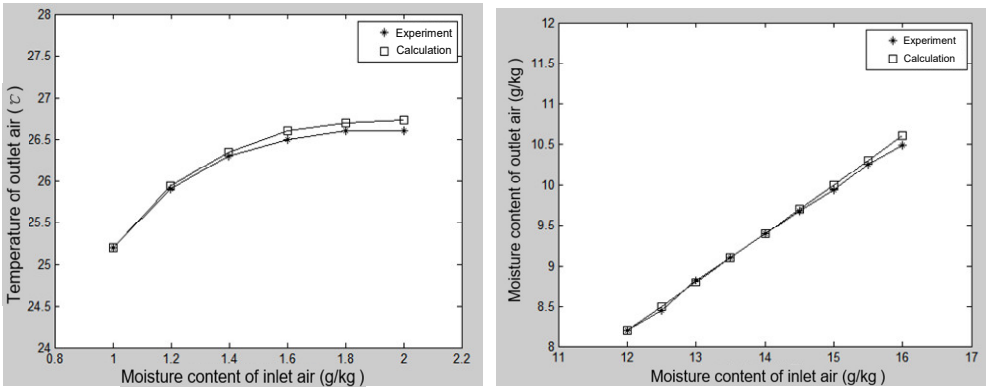

Figure 17. Comparison of calculated and experimental values of moisture content of outlet air.

4.2. Comparison of Outlet Temperature of Treated Air

In the processing area, as the temperature of the rotor adsorbent leaving the regeneration area is higher than the inlet temperature of the processing air, the heat transfer effect and the adsorption heat released when the water vapor is adsorbed make the temperature of the adsorbent continue to decrease and the outlet temperature of the processing air continue to increase. The increase in the moisture content of the inlet air will accelerate the adsorption rate, and the release of the adsorption heat causes the outlet air temperature to increase. From the data in Figure 18, the deviation between the calculated value and the experimental value of the outlet air temperature is 3.03%.

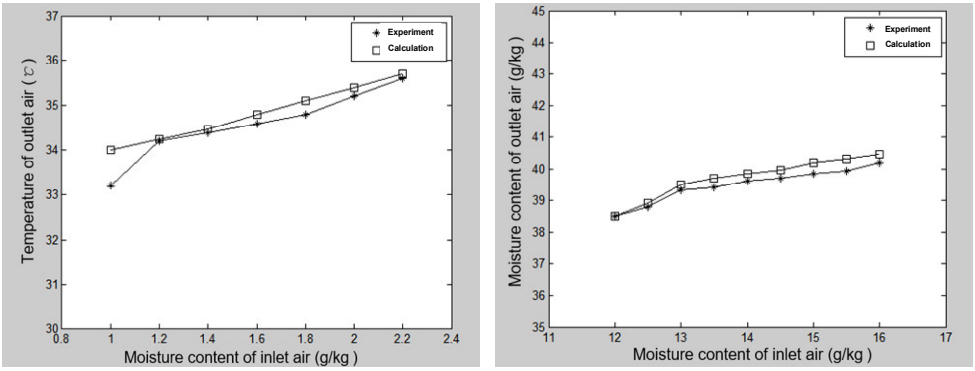

Figure 18. Comparison of calculated and experimental values of exit air temperature.

4.3. Comparison of Water Intake

By comparing the adsorption amount of desiccant calculated by a simulation with the actual water intake in the experiment, it can be seen from the data in Figure 19 that when the inlet air moisture content is 2 g/kg, the deviation between the calculated value and the experimental value is 8.23%.

In summary, the agreement between the theoretical calculation data and the experimentally obtained data is good, indicating that the mathematical model of dehumidification of the rotor established in this paper is correct, and the parameter optimization method is effective.

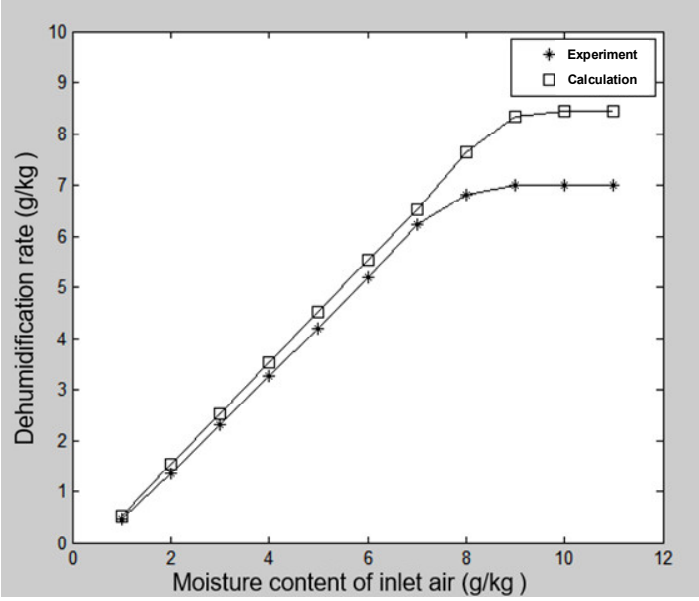

Figure 19. Comparison between calculated and experimental values of desiccant capacity of runner.

5. Discussion

The optimized product can achieve a maximum water intake of 15.8 Kg/h at an average humidity of 1.3 g/Kg and 75 Kg/h at an average relative humidity of 96%. The following conclusions can be drawn from the study of this project:

1. Increasing the thickness of the runner is beneficial to improving its hygroscopicity/desorption capacity, and the thickness of the runner determines the optimal speed and regeneration angle;
2. The temperature of regenerated air has an important effect on the desorption efficiency and the DCOP, and the humidity of the regenerated air has little effect on the wettability of the runner;
3. The moisture absorption D and DCOP of the runner are inversely proportional to the temperature of the treated air and directly proportional to the humidity;
4. The system design and the control of rotor parameters and air parameters can effectively increase water extraction.

6. Conclusions

In order to improve the efficiency of air water intake, in addition to the improvement of the performance of the adsorbent material, subsequent research is required in the following areas:

(1) The study of the partition ratio of the processing area and the regeneration area of the rotor. If the ratio of the processing area is too large, the moisture adsorbed by the absorbent cannot be fully carried away by the regeneration air. If the ratio of the processing area is too small, the moisture adsorbed by the absorbent is not enough to become saturated wet air, both of which reduce the utilization rate of the rotor.

(2) Regeneration heating temperature determination. If the regeneration temperature is too high, it will lead to the increased energy consumption of the entire system; if the regeneration temperature is too low, this will lead to desorption not being complete. The regeneration temperature is determined by and directly related to the division of the rotor area, the moisture absorption material selection, etc., and any change in the regeneration temperature will need to change correspondingly.

At the same time, the energy integration design of vehicle and water intake equipment is also one of the important research directions to improve water intake efficiency.

Author Contributions: Conceptualization, G.L. and Y.H.; methodology, Y.H. and G.L.; software, Y.H. and W.Z.; validation, Y.H., G.L. and R.Z.; investigation, Y.H. and G.L.; resources, G.L.; data curation, Y.H., H.B. and W.Z.; writing—original draft preparation, Y.H., H.B. and W.Z.; writing—review and editing, Y.H., H.B., G.L., R.Z. and W.Z.; visualization, Y.H. and W.Z.; supervision, G.L.; project administration, G.L.; funding acquisition, G.L. All authors have read and agreed to the published version of the manuscript.

Funding: This research received no external funding.

Data Availability Statement: The study did not report any data.

Acknowledgments: We would like to sincerely thank all of our previous and current teachers and classmates who laid the basis for this research.

Conflicts of Interest: The authors declare no conflict of interest.

References

1. Biswas, A.K.; Tortajada, C. Water crisis and water wars: Myths and realities. *Int. J. Water Resour. Dev.* **2019**, *35*, 727–731. [CrossRef]
2. Salehi, A.A.; Ghannadi-Maragheh, M.; Torab-Mostaedi, M.; Torkaman, R.; Asadollahzadeh, M. A review on the water-energy nexus for drinking water production from humid air. *Renew. Sustain. Energy Rev.* **2020**, *120*, 109627. [CrossRef]
3. Tu, R.; Hwang, Y. Reviews of atmospheric water harvesting technologies. *Energy* **2020**, *201*, 117630. [CrossRef]
4. Patel, J.; Patel, K.; Mudgal, A.; Panchal, H.; Sadasivuni, K.K. Experimental investigations of atmospheric water extraction device under different climatic conditions. *Sustain. Energy Technol. Assess.* **2020**, *38*, 100677. [CrossRef]
5. Kandeal, A.W.; Joseph, A.; Elsharkawy, M.; Elkadeem, M.R.; Hamada, M.A.; Khalil, A.; Moustapha, M.E.; Sharshir, S.W. Research progress on recent technologies of water harvesting from atmospheric air: A detailed review. *Sustain. Energy Technol. Assess.* **2022**, *52*, 102000. [CrossRef]
6. Shafeian, N.; Ranjbar, A.A.; Gorji, T.B. Progress in atmospheric water generation systems: A review. *Renew. Sustain. Energy Rev.* **2022**, *161*, 112325. [CrossRef]
7. Raveesh, G.; Goyal, R.; Tyagi, S.K. Advances in atmospheric water generation technologies. *Energy Convers. Manag.* **2021**, *239*, 114226. [CrossRef]
8. Toribio, F.; Bellat, J.P.; Nguyen, P.H.; Dupont, M. Adsorption of water vapor by poly (styrenesulfonic acid), sodium salt: Isothermal and isobaric adsorption equilibria. *J. Colloid Interface Sci.* **2004**, *280*, 315–321. [CrossRef] [PubMed]
9. Seo, Y.K.; Yoon, J.W.; Lee, J.S.; Hwang, Y.K.; Jun, C.H.; Chang, J.S.; Wuttke, S.; Bazin, P.; Vimont, A.; Daturi, M.; et al. Energy-efficient dehumidification over hierachically porous metal–organic frameworks as advanced water adsorbents. *Adv. Mater.* **2012**, *24*, 806–810. [CrossRef] [PubMed]
10. Tao, P.; Liao, B.; Tan, Y. A primary study on the water absorbing/releasing performance of molecular sieve desiccant. *Procedia Eng.* **2012**, *27*, 781–786. [CrossRef]
11. Hao, X.; Geng, S.; Yuan, L.; Luo, B. Study of composite scheme of absorption/desorption method and condensation method for extracting water from air. *Procedia Eng.* **2017**, *205*, 2069–2075. [CrossRef]
12. Zhang, T.; Liu, X.H.; Zhang, L.; Jiang, Y. Match properties of heat transfer and coupled heat and mass transfer processes in air-conditioning system. *Energy Convers. Manag.* **2012**, *59*, 103–113. [CrossRef]
13. Ge, T.S.; Li, Y.; Wang, R.Z.; Dai, Y.J. A review of the mathematical models for predicting rotary desiccant wheel. *Renew. Sustain. Energy Rev.* **2008**, *12*, 1485–1528. [CrossRef]
14. Zhang, X.J.; Dai, Y.J.; Wang, R.Z. A simulation study of heat and mass transfer in a honeycombed rotary desiccant dehumidifier. *Appl. Therm. Eng.* **2003**, *23*, 989–1003. [CrossRef]
15. Hao, H.; Song, X.Y.; Xin, P. Study on the adsorption and purification performance of runner with different staged regeneration modes. In *IOP Conference Series: Materials Science and Engineering*; IOP Publishing: Brașov, Romania, 2020; Volume 789, p. 012025.
16. Eslami, M.; Tajeddini, F.; Etaati, N. Thermal analysis and optimization of a system for water harvesting from humid air using thermoelectric coolers. *Energy Convers. Manag.* **2018**, *174*, 417–429. [CrossRef]
17. Chen, Z.; Song, S.; Ma, B.; Li, Y.; Shao, Y.; Shi, J.; Liu, M.; Jin, H.; Jing, D. Recent progress on sorption/desorption-based atmospheric water harvesting powered by solar energy. *Sol. Energy Mater. Sol. Cells* **2021**, *230*, 111233. [CrossRef]
18. Kim, H.; Yang, S.; Rao, S.R.; Narayanan, S.; Kapustin, E.A.; Furukawa, H.; Umans, A.S.; Yaghi, O.M.; Wang, E.N. Water harvesting from air with metal-organic frameworks powered by natural sunlight. *Science* **2017**, *356*, 430–434. [CrossRef] [PubMed]
19. Abdelgaied, M.; Kabeel, A.E.; Zakaria, Y. Performance improvement of desiccant air conditioner coupled with humidification-dehumidification desalination unit using solar reheating of regeneration air. *Energy Convers. Manag.* **2019**, *198*, 111808. [CrossRef]
20. Ge, T.S.; Dai, Y.J.; Wang, R.Z. Review on solar powered rotary desiccant wheel cooling system. *Renew. Sustain. Energy Rev.* **2014**, *39*, 476–497. [CrossRef]

21. Pang, Y.F. The theoretical analysis and experimental research on the optimal condition of semiconductor refrigeration. In *IOP Conference Series: Earth and Environmental Science*; IOP Publishing: Beijing, China, 2016; Volume 40, p. 012013.
22. Wei, X.; Chai, Z.; Fang, L.; Luo, M.; Gou, M.; Zhen, X. Experiment of Solar Semiconductor Condensing Wall Water Intake System Based on Big Data. In *Journal of Physics: Conference Series*; IOP Publishing: Hubei, China, 2021; Volume 2138, p. 012022.

Disclaimer/Publisher's Note: The statements, opinions and data contained in all publications are solely those of the individual author(s) and contributor(s) and not of MDPI and/or the editor(s). MDPI and/or the editor(s) disclaim responsibility for any injury to people or property resulting from any ideas, methods, instructions or products referred to in the content.